Indian Journal of Chemical Technology
Vol. 30, November 2023, pp. 812-821
DOI: 10.56042/ijct.v30i6.6546

Removal of methylene blue dye from aqueous media by adsorption using nickel oxide modified montmorillonite composite

H Boukhatem[1]*, N Ouazene[2], H Rezala[1], L Djouadi[3], S Selami[1] & S Zeraif[1]

[1]Université Djilali BOUNAAMA de Khemis-Miliana, Faculté des Sciences et de la Technologie, Route de Theniet El Had, 44225 Khemis-Miliana, Algérie

[2]Laboratoire Sciences et Techniques de l'Environnement, Ecole Nationale Polytechnique d'Alger, BP 182, El Harrach, Alger, Algérie

[3]Laboratoire de Génie Chimique, Département de Génie des procédés, Faculté de Technologie, Université Saad Dahleb-Blida 1, BP270-09000-Blida, Algérie

*E-mail: boukhatem_houria@yahoo.fr

Received 19 August 2022; accepted 5 September 2023

In this study, the adsorptive removal of methylene blue (MB) from aqueous solutions onto nickel oxide (NiO) modified montmorillonite (NiO-Mt) has been studied and compared with that of commercial bentonite. The influences of various experimental factors such as contact time, adsorbent dosage, pH of solution, initial dye concentration and temperature have been investigated. Batch adsorption studies has manifested that the maximum adsorption capacity of MB is around 99.9 mg/g in 10 min with 25 mg adsorbent mass at an initial concentration of 100 mg/L at ambient temperature of 25°C and natural pH of solution (pH = 5.8 for NiO-Mt and pH = 6.3 for commercial bentonite). The adsorption kinetics and isotherms are well fitted by pseudo-second order and Langmuir models, respectively. The thermodynamic parameters such as the changes in Gibbs free energy, enthalpy, and entropy are determined. The MB adsorption is physical, spontaneous and exothermic for both adsorbents.

Keywords: Adsorption, Isotherms, Kinetics, Methylene blue, NiO-Mt, Thermodynamics

Dyes are commonly used in textile, paper, plastic, leather, cosmetic, pharmaceutical and food industries[1-4]. The discharge of dye wastewaters directly into rivers and lakes, even at very low concentrations, can endanger the living organisms and its aquatic ecology because of their toxicity due to the aromatic structures. Dye accumulation in water reduces the sunlight penetration, which harms the photosynthesis activity of aquatic plants. Methylene blue (MB) is a cationic dye and considered as the most commonly used dye in industry[5]. Its long-term exposure can cause vomiting, nausea, anemia, hypertension and heart rate increasing[5-7]. Therefore, the treatment of dyeing wastewater is an important topic of research and one of the difficult challenges.

Recently, many techniques such as ion exchange, adsorption, membrane filtration, coagulation/ flocculation and hybrid flotation have been employed for the removal of dyes from aqueous solutions[8-10]. The use of these methods has been limited due to their high capital and operating costs. Among all treatment processes, adsorption has been proven more attractive and effective due to higher efficiency, lower cost, simplicity of operation and lower sensitivity to toxic pollutants[4].

Activated carbon is the most efficient adsorbent used for dye removal. However, it is expensive to produce and difficult to regenerate after use[11-14]. Therefore, research on alternative adsorbents with high removal capacity is required. The clays have been increasingly receiving attention because they are abundant, cheap, easy to handle, and highly efficient[2, 15]. Modification of different clay types using various kinds of chemical modifying agents for removing various organic compounds from water has been widely studied[16-26].

In this study, we employed NiO for mont-morillonite modification by hydrothermal synthesis method as a novel composite with enhanced adsorption properties and affinity to MB dye, and compared with a commercial bentonite. The two samples were characterized through Fourier Transform Infrared Spectroscopy (FTIR), X-ray fluorescence (XRF) and X-ray diffraction (XRD) techniques. The effects of various operating parameters on adsorption such as contact time,

adsorbent mass, solution pH, initial dye concentration and temperature were investigated in controlled batch experiments. Furthermore, kinetics, thermodynamic studies and equilibrium isotherms were conducted to evaluate the experimental data.

Experimental Section

Materials

The Na-montmorillonite (Na-Mt) was obtained by purification of an Algerian raw bentonite according to a previously reported procedure[27]. Commercial bentonite, nickel nitrate hexahydrate ($Ni(NO_3)_2.6H_2O$), sodium carbonate (Na_2CO_3), hydrochloric acid (HCl), sodium chloride (NaCl), sulfuric acid (H_2SO_4) and methylene blue ($C_{16}H_{18}ClN_3S$) were purchased from Biochem Chemopharma. Sodium hydroxide (NaOH) was purchased from Panreac. All reagents were used as received without further purification. All solutions were prepared in distilled water.

Preparation of nickel oxide-montmorillonite (NiO-Mt)

5 g of Na-Mt was dispersed in 500 mL of distilled water under stirring for a night. Then 100 mL of sodium carbonate solution (0.025 mol/L) was mixed dropwise with Na-Mt suspension under stirring for 3 h followed by addition of 100 mL of nickel nitrate solution (0.025 mol/L) dropwise under continuous stirring for a night.

After that, the mixture was autoclaved at 100°C for 1 h. After the synthesis period, the sample was separated and washed with distilled water for several times, and then dried at 100°C. Finally, the collected solid was referred to as NiO-Mt for further characterization and application.

Characterization

The active groups were studied by FTIR using an IRTracer-100 SHIMADZU spectrometer controlled by a computer equipped with specialised software for acquiring and processing results in the range 400 - 4000 cm^{-1}. The sample was prepared by mixing an amount of material powder with KBr. The mixture was compressed under vacuum at room temperature into a pellet ready for analysis. The chemical composition of materials was determined by X-ray fluorescence spectrometry using the ZSX Primus II RIGAKU spectrometer, equipped with an Rh tube and controlled by a computer. The detection range is from B (Boron) to U (Uranium), in the order of ppm at 100%. The sample to be analyzed was compressed into a 1 g pellet. The powder XRD patterns were recorded by RIGAKU diffractometer with Cu kα radiation (1.5406 Å, 40 mV, 40 A) at a step size of 0.01° and a 2θ between 2 to 70°.

The point of zero charge tests of the two samples (NiO-Mt and commercial bentonite) were carried out as follows: 20 mL of 0.01 mol/L NaCl solution was placed in flasks. The pH was adjusted to a value between 3 and 9 by addition of H_2SO_4 (0.1 mol/L) or NaOH (0.1 mol/L). The NiO-Mt or commercial bentonite (0.04 g) was added to the solution and the flasks were shaken at 150 rpm for 24 h at room temperature, centrifuged and the final pH was measured and plotted against the initial pH. As reported elsewhere[28], the pH at which the curve crossed the line, $pH_{initial} = pH_{final}$, was taken as the point of zero charge, pH_{PZC}.

Adsorption studies

Effect of contact time was investigated by contacting 25 mg of commercial bentonite or NiO-Mt with 25 mL of MB solution with initial concentration of 100 mg/L at natural pH of the solution in flasks, and were shaken in a shaker (Memmert) at 150 rpm for certain time intervals (5 - 90 min). After the process was completed, the mixtures were centrifuged at 3200 rpm for 10 min to separate the solution from the adsorbents. The concentration of MB solution was measured quantitatively with spectrophotometer (UV-2005 SELECTAP) at the maximum wavelength (665 nm). The adsorption capacity (Q_e) was calculated using:

$$Q_e = \frac{(C_0 - C_e)V}{m} \quad \ldots(1)$$

Where Q_e is the amount of MB adsorbed at equilibrium (mg/g), C_0 and C_e (mg/L) are the liquid phase concentrations of MB at initial and equilibrium, respectively. V is the volume of methylene blue solution (L) and m is the mass of adsorbents used (g). To determine the adsorbent dosage, various mass (10, 15, 20, 25, 30, and 40 mg) of commercial bentonite or NiO-Mt were dispersed into 25 mL of MB solution with initial concentration of 100 mg/L. Each dispersion was shaked for 10 min at ambient temperature (25°C) and natural pH of the solution.

The influence of pH on the adsorption was studied at pH ranging from 3 to 11. 25 mg of each adsorbent were added to MB solutions with initial concentration of 100 mg/L and a volume of 25 mL. The mixtures were shaken for 10 min. Effect of dye initial concentration was performed at 25°C by mixing

25 mg of commercial bentonite or NiO-Mt with 25 mL solution (natural pH of the solutions) of definite concentration of MB (30 – 300 mg/L) for 10 min of shaking. Effect of temperature was examined by MB adsorption at different temperatures 25, 30, 35, 40 and 50°C at natural pH of the solutions and 25 mg as adsorbent mass.

Results and Discussion

Characterization of the adsorbents

FTIR

The identification of some characteristic functional groups was investigated using the FTIR technique and the spectra of the samples are illustrated in Fig. 1. The observed peak at 3630 cm^{-1} is corresponding to the stretching vibrations of –OH groups of Al–OH[29, 30]. The broad absorption band centered at 3440 cm^{-1} is attributed to the characteristic surficial silanol group (SiO–H)[31, 32]. The peak at approximately 1640 cm^{-1} is assigned to the bending vibrations of O–H in adsorbed water molecules[30, 33-35]. The intense band centered at 1030 cm^{-1} is ascribed to the asymmetric Si–O–Si stretching vibrations of the tetrahedral sheet[29-31, 36, 37]. The peak at 910 cm^{-1} is due to the hydroxide (OH) deformation linked to Al and/or Mg ions[38]. The bands at 530 and 470 cm^{-1} were due to Si–O–Al and Si–O–Si bending vibrations, respectively[29]. The peak at 1390 cm^{-1} is characteristic of NiO[39].

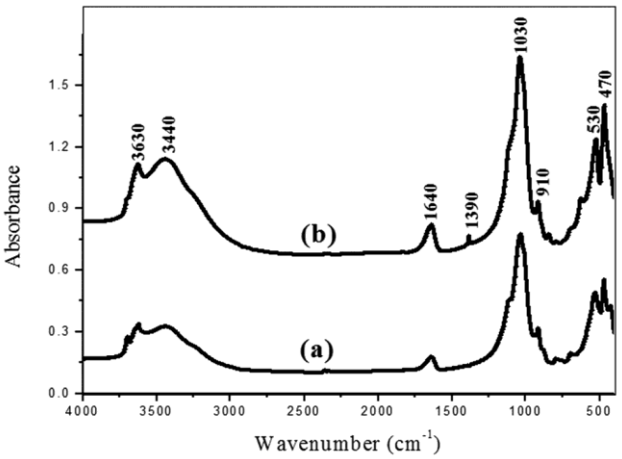

Fig. 1 — FTIR spectra of (a) commercial bentonite and (b) NiO-Mt

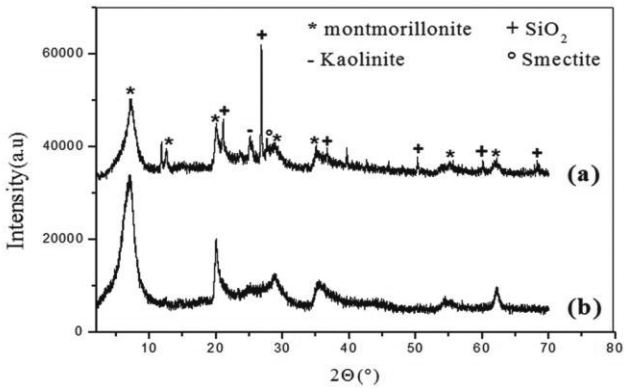

Fig. 2 — XRD patterns of (a) commercial bentonite and (b) NiO-Mt

XRF

The compositional analysis was carried out to find the chemical compositions of the clay samples. The results of XRF of both materials are shown in Table 1. Major quantities of SiO_2 and Al_2O_3 are present in both samples, indicating that these clays belong to aluminosilicate materials. The red colour of commercial bentonite is due to the high concentration of Fe_2O_3 (20.43 wt%). The amount of Na_2O in the NiO-Mt sample decreased after the modification process of Na-Mt (Supplementary data (Table S1)) due to the cation exchange between Na^+ and Ni^{2+}.

Table 1 — X-ray fluorescence analysis of commercial bentonite and NiO-Mt

Oxide	(Wt. %)	
	NiO-Mt	commercial bentonite
Na_2O	1.802	1.970
MgO	4.218	2.396
Al_2O_3	22.119	18.868
SiO_2	55.307	47.798
K_2O	0.222	1.089
CaO	0.261	1.351
MnO	0.083	0.107
Fe_2O_3	4.996	20.435
NiO	10.786	0.077
SO_3	/	0.579
TiO_2	/	3.705
Others	0.183	0.305

XRD

The XRD patterns of the commercial bentonite and NiO-Mt are shown in Fig. 2. From Fig. 2a, it can be seen that the commercial bentonite is consisted of montmorillonite, smectite, kaolinite and SiO_2. The characteristic diffraction peaks of montmorillonite are at 7.0, 12.5, 19.7, 28.7, 34.8, 55.3 and 62.2° [40-42], while those of kaolinite and smectite at 25.0 and 27.7°, respectively[42], and those of SiO_2 at 20.9, 26.8, 36.8, 50.2, 60.0 and 68.0° [42].

The NiO-Mt (Fig. 2b) inherited the diffraction peaks of montmorillonite, suggesting that the clay

structure preserved well enough after the modification. The low intensity diffraction peaks at 14.2 and 44.5° in Na-Mt (Supplementary Information**,** Fig. S1) disappeared in NiO-Mt, indicating the high dispersion of NiO on NiO-Mt adsorbent surface.

No diffraction attributed to NiO can be observed in the pattern of the NiO-Mt adsorbent due to the amorphous state of NiO or the high dispersion of NiO on the adsorbent surface. This is in line with Faezeh Farzaneh et al.[43]. The authors reported that at room temperature up to 200°C amorphous phases were formed, while metal oxide crystallization occurred after heat treatment at 200°C. By increasing the temperature up to 300°C and 400°C the NiO as a crystalline phase is observed.

Adsorption of methylene blue

Effect of contact time and kinetic studies

The effect of contact time on adsorption of organic molecules is an important factor to determine the equilibrium time. The adsorbed MB amount by commercial bentonite and NiO-Mt versus the contact time is shown in Fig. 3. With increasing time, the adsorption process proceeds through two stages. The removal was fast in the first stage (from 0 to 10 min) because all adsorbent sites are vacant and there was higher concentration of MB in solution. In the second stage (from 10 to 90 min), the dye adsorption amount remained unchanged with the increase of contact time because the adsorption sites were occupied and the dye concentration decreased. From Fig. 3, it can be seen that the equilibrium was reached in 10 min with an adsorbed amount of 99.9 mg/g when the MB initial concentration was 100 mg/L for both adsorbents.

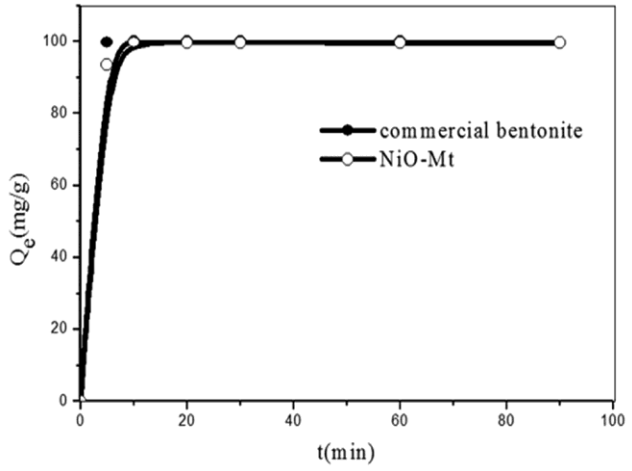

Fig. 3 — Effect of contact time on MB adsorption by commercial bentonite and NiO-Mt

Several other modified clays have yielded similar results[3, 44-48]. Therefore, the contact time of 10 min was used in subsequent experiments.

Adsorption kinetics is essential in the evaluation of adsorbents for dye removal from aqueous solutions. The most commonly used adsorption kinetics models are the Lagergren pseudo-first-order and pseudo-second-order kinetic models. The pseudo-first-order kinetic equation is expressed as follows[49, 50]:

$$\frac{dQ_t}{dt} = K_1 (Q_e - Q_t) \quad \text{... (2)}$$

It can be expressed in linear form:

$$\mathrm{Log}(Q_e - Q_t) = \mathrm{Log}Q_e - \frac{K_1}{2.303} t \quad \text{... (3)}$$

Where Q_t and Q_e are the adsorbed amounts (mg/g) of MB at time t and equilibrium, respectively, and K_1 is the rate constant of pseudo-first-order adsorption (min^{-1}). A plot of Log ($Q_e - Q_t$) versus t gives a linear relationship, from which the values of K_1 and Q_e can be determined from the slope and intercept.

The pseudo-second-order kinetics may be expressed as[49, 50]

$$\frac{dQ_t}{dt} = K_2 (Q_e - Q_t)^2 \quad \text{... (4)}$$

It can be expressed in linear form :

$$\frac{t}{Q_t} = \frac{1}{K_2 Q_e^2} + \frac{1}{Q_e} t \quad \text{... (5)}$$

Where K_2 is the pseudo second-order rate constant of adsorption (g/mg.min). The slope and intercept of the linear plot t/Q_t versus t yield the value of Q_e and k_2.

Kinetic parameters were collected in Table 2. From Table 2, it can be seen that the determination coefficients (R^2) of the pseudo-second order model were higher than that of the pseudo-first order model. Moreover, the calculated ($Q_{e,cal}$) values using pseudo-second order kinetic model are closer to the experimental data ($Q_{e,exp}$) while those calculated from pseudo-first order model largely deviate from ($Q_{e,exp}$). The results indicated that the adsorption of MB by commercial bentonite and NiO-Mt accorded with the pseudo-second-order model. This model describes adsorption kinetics taking into account both the case of rapid fixation of solutes on the most reactive sites, and that of slow fixation to low energy sites.

Effect of adsorbent dosage

Adsorbent mass is another critical parameter in the study of adsorption in order to determine the most

Table 2 — Pseudo-first order and pseudo-second order kinetic model parameters for MB adsorption by commercial bentonite and NiO-Mt

Model	Parameters	NiO-Mt	commercial bentonite
Pseudo-first order	$Q_{e,exp}$(mg/g)	99.8930	99.9153
	Q_e(mg/g)	4.8424	0.5716
	K_1(min^{-1})	0.0507	0.0366
	R^2	0.2557	0.1473
Pseudo-second order	Q_e(mg/g)	99.8004	99.8004
	K_2(g/mg.min)	0.0956	0.4974
	R^2	0.9999	1

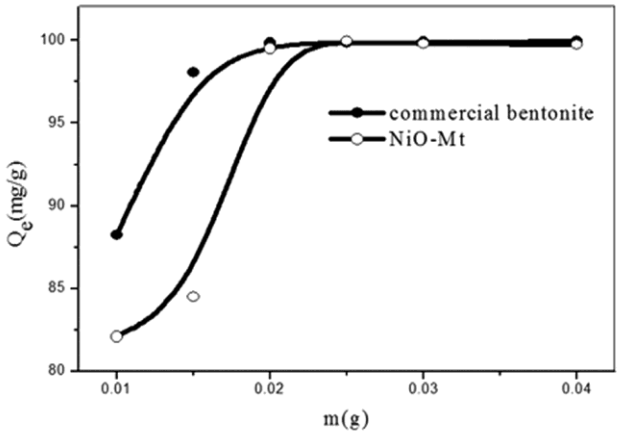

Fig. 4 — Effect of adsorbent mass on MB adsorption by commercial bentonite and NiO-Mt

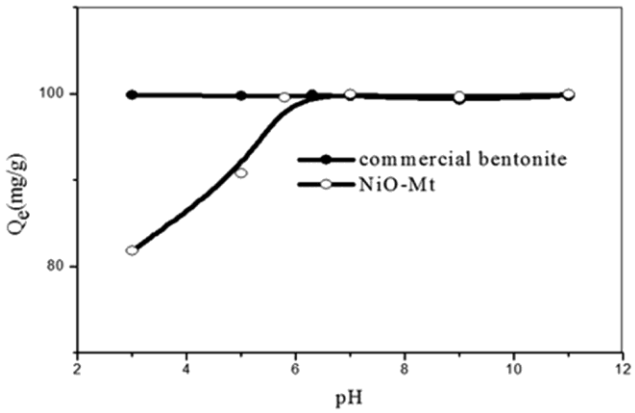

Fig. 5 — Effect of solution pH on MB adsorption by commercial bentonite and NiO-Mt

economical amount of adsorbent that can effectively remove the target chemical species from wastewater. Fig. 4 shows the effect of adsorbent mass on the MB adsorption capacity. The adsorbed amount of MB increased sharply with an increase in the adsorbent mass from 0.01 to 0.025 g. This may be due to the availability of more adsorption sites. However, further increase in adsorbent mass over to 0.025 g, the adsorbed dye amount tried to maintain a stable progression which may be due to equilibrium establishment at an extremely low MB concentration in the adsorption medium[5, 51, 52]. Hence, the optimal adsorbent mass of 25 mg was chosen for both adsorbents to carry out the next adsorption experiments.

Effect of solution pH

Solution pH is an essential parameter in adsorption studies as it affects the surface charge of the adsorbent, and the degree of ionization and speciation of the adsorbate [9, 53]. Fig. 5 shows the effect of pH on the adsorption capacity of MB onto both adsorbents. In this study, changes in pH solution had no significant influence on the adsorbed amount of commercial bentonite. Narine and Guy[54] have reported that the adsorption capacity of bentonite was essentially independent of pH in the range 4.5 – 8.5. Similar results were obtained for the adsorption of MB by bentonite and sepiolite[55] and Na-Mt[56]. For NiO-Mt, the adsorbed amount of MB has been found to be dependent on pH of the solution. The adsorption capacity increases with increasing pH over the range of 3 – 5.8. However, the adsorption capacity tended to have stability when pH is between 5.8 and 11. Similar results were reported previously [4, 7, 57, 58].

To evaluate the effect of pH on the MB adsorption, the point of zero charge (pH_{PZC}) of the adsorbents must be investigated. The values of pH_{PZC} of commercial bentonite and NiO-Mt were found as 7.5 and 6.8, respectively, as shown in Fig. 6. Hence, the surface charge was positively or negatively charged when the solution pH was less or more than the pH_{PZC}, repectively. MB has a pKa = 3.8[59]. When the pH<pKa, MB mostly exist as undissociated (neutral) molecules. Whereas when the pH>pKa, MB mostly exist as cationic species. Therefore, The highest MB removal found at pH<7.5 for commercial bentonite is due to the hydrogen bonding interaction between the imines groups of MB molecules and the silanol groups of the commercial bentonite. In the

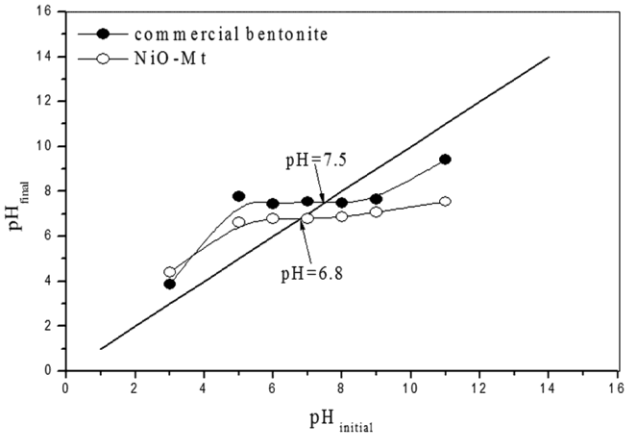

Fig. 6 —Determination of the pH_{PZC} for commercial bentonite and NiO-Mt

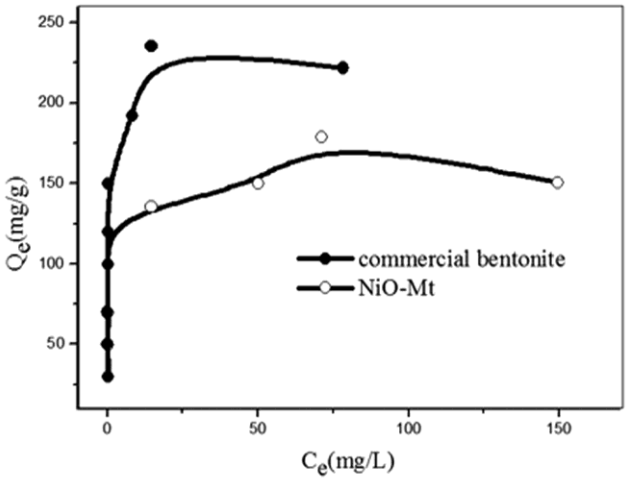

Fig. 7 — Isotherms for MB adsorption by commercial bentonite and NiO-Mt

case of NiO-Mt, the lowest removal of MB at pH<6.8 is attributed to the presence of excess H^+ ions competing with the dye cations for adsorption sites and the electrostatic repulsion between the positively charged surface of adsorbent and positively charged MB cations.

At pH>7.5 (pH>6.8) for commercial bentonite (NiO-Mt), the surface of both adsorbents becomes more negative. Additionally, the silanol groups on the adsorbents surface also become increasingly deprotonated at higher pH values. So, the number of negative charges on the adsorbents surface increased, and two probable mechanisms of MB adsorption could be occurred with increasing pH. The first is the strong electrostatic attraction occurred between negatively charged groups on the adsorbents and positively charged MB cations. The second is the hydrogen bonding interaction between the imines groups of MB molecules and the silanol groups of the adsorbents. Natural pH solutions (5.8 for NiO-Mt and 6.3 for commercial bentonite) were selected as the optimum conditions for adsorption of MB on the surface of the investigated adsorbents. So, the pH of the MB solution was not adjusted in the subsequent isotherm and temperature experiments.

Effect of initial MB concentration and adsorption isotherms

The effect of dye concentration on the adsorption was investigated by varying the initial MB concentration from 30 to 300 mg/L (Fig. 7). In Fig. 7, the adsorbed amount of MB increased quickly with the initial dye concentration from 30 to 200 mg/L and 30 to 120 mg/L for commercial bentonite and NiO-Mt, respectively. However, no noticeable increase in adsorption capacity can be observed in the concentration range of 200 – 300 mg/L and 120 – 300 mg/L for commercial bentonite and NiO-Mt, respectively. At low concentrations, there will be unoccupied active sites on the adsorbent surface. At high concentrations there will be a deficiency in the active sites required for the adsorption of the overall MB molecules due to its saturation[7, 60]. The Q_{max} values from the experimental results are 150.54 mg/g and 221.82 mg/g for NiO-Mt and commercial bentonite, respectively, which is due to the presence of more actif sites on commercial bentonite surface than NiO-Mt. Commercial bentonite gives better results, but those abtained by NiO-Mt were also considerable. This study offers enough proof that local modified montmorillonite (NiO-Mt) is efficient in the removal of methylene blue from aqueous solutions. This is an important economic reason from the perspective of scaling up productions for industrial applications instead to import foreign adsorbents (commercial bentonite). Furthermore, using low masses of NiO-Mt with shortest adsorption time is economically more favorable.

The adsorption isotherm is important to illustrate the distribution of adsorbate molecules between the liquid and solid phases when the adsorption reaches equilibrium[12, 61, 62]. Adsorption isotherms describe the relationship of the equilibrium adsorbed quantity (Q_e) with the equilibrium concentration (C_e) under a certain temperature.

In this study, the adsorption isotherm data were fitted using two well-known adsorption equations, Langmuir and Freundlich models. The Langmuir equation is given as follows[63]:

$$\frac{C_e}{Q_e} = \frac{1}{Q_m} C_e + \frac{1}{Q_m K_L} \quad \text{... (6)}$$

where Q_e is the amount of dye adsorbed on the adsorbent (mg/g) at equilibrium, C_e is the equilibrium dye concentration in solution (mg/L), Q_m is the maximum adsorption amount for the adsorbent (mg/g) and K_L is the Langmuir adsorption constant (L/mg). The constants Q_m and K_L were determined from the slope and intercept of the linear plots of the experimental data of C_e/Q_e versus C_e, respectively. The Freundlich isotherm model is given by the following equation[63]:

$$\mathrm{Log}Q_e = \mathrm{Log}K_f + \frac{1}{n}\mathrm{Log}C_e \quad \text{... (7)}$$

Where Q_e is the adsorbed amount of dye per unit mass of adsorbent (mg/g), C_e is the equilibrium concentration of dye in solution (mg/L) and K_f and n are Freundlich constants. A plot of $\mathrm{Log}Q_e$ versus $\mathrm{Log}C_e$ enables the empirical constants K_f and 1/n to be determined from the intercept and slope of the linear regression. The Freundlich and Langmuir model parameters determined from Fig. 8 are listed in Table 3.

The determination coefficients for Langmuir isotherm were highest in comparison with the values obtained for Freundlich isotherm. Therefore, Langmuir isotherm in both cases provides a better fit for experimental data. The Langmuir theory assumes that adsorption occurs at specific homogenous sites within the adsorbent and that once a dye molecule occupies a site, no further adsorption can occur at that site. The maximum adsorption capacity was estimated to be 154.32 mg/g and 222.71 mg/g for NiO-Mt and commercial bentonite, respectively, which is in agreement with the experimental results obtained from the isotherm curves.

Effect of temperature and thermodynamic studies

Temperature is one of the most important factors in the adsorption process. The influence of temperature was done at various temperatures (25, 30, 35, 40 and 50°C) and given in Fig. 9. The best results were found at ambient temperature (25°C) and the adsorbed amount of MB decreased slowly at higher temperature (50°C), indicating that the MB adsorption in this system was exothermic and suggesting the weakening of the bond between adsorbents and MB molecules with the increase of temperature, which reduce the MB elimination. Similar trend was observed for the adsorption of MB by bentonite and alginate beads[2].

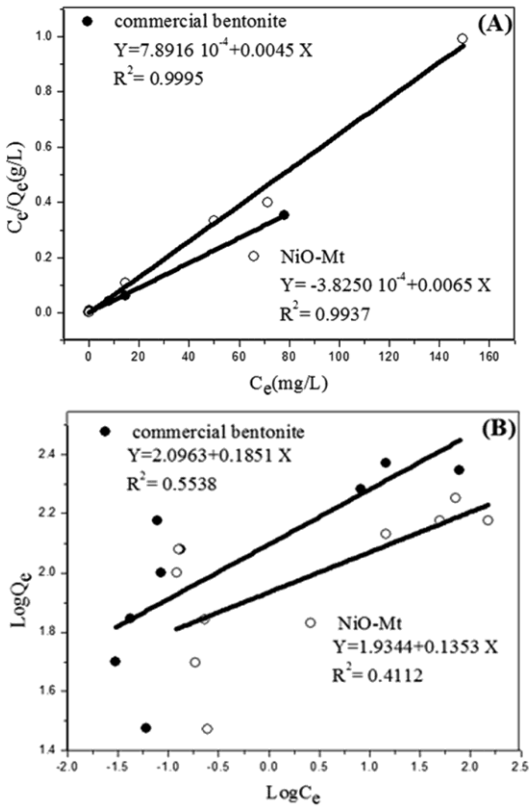

Fig. 8 — Linear (a) Langmuir and (b) Freundlich plots for MB adsorption by commercial bentonite and NiO-Mt

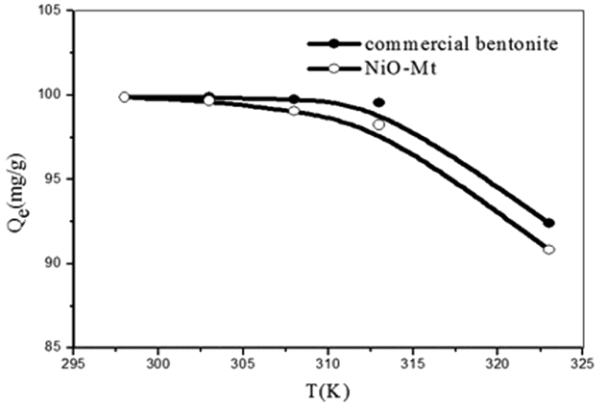

Fig. 9 — Effect of temperature on MB adsorption by commercial bentonite and NiO-Mt

Table 3 — Langmuir and Freundlich isotherm parameters for MB adsorption by commercial bentonite and NiO-Mt

Model	Parameters	NiO-Mt	commercial bentonite
Langmuir	K_L (L/mg)	16.9412	5.6896
	Q_m (mg/g)	154.3210	222.7171
	R^2	0.9937	0.9995
Freundlich	1/n	0.1353	0.1851
	K_f (mg/g)	85.9785	124.8130
	R^2	0.4112	0.5538

Table 4 — Thermodynamic parameters for MB adsorption by commercial bentonite and NiO-Mt

Adsorbent	ΔH° (kJ/mol)	ΔS° (J/mol.K)	R^2	ΔG° (kJ/mol)				
				298K	303K	308K	313K	323K
NiO-Mt	-138.9421	-411.1756	0.9957	-16.4118	-14.3559	-12.3000	-10.2441	-6.1324
commercial bentonite	-146.8679	-429.5948	0.8984	-18.8487	-16.7001	-14.5327	-12.4048	-8.1088

The adsorption process is often accompanied by thermal effects; therefore, the study of thermodynamic parameters of adsorption is essential. The thermodynamic parameters evaluated for MB adsorption onto commercial bentonite and NiO-Mt are the free energy change (ΔG°), enthalpy change (ΔH°) and entropy change (ΔS°). These parameters were calculated using the following equations[7]:

$$K_c = \frac{Q_e}{C_e} \quad \ldots(8)$$

$$LnK_c = \frac{\Delta S^0}{R} - \frac{\Delta H^0}{RT} \quad \ldots(9)$$

$$\Delta G^0 = \Delta H^0 - T\Delta S^0 \quad \ldots(10)$$

where K_c is the thermodynamic equilibrium constant, T is the temperature at which the experiment is performed, and R is the universal gas constant (8.314 J/mol.K).

The values of ΔH° and ΔS° were calculated from slope and intercept of van't Hoff scheme of LnK_c against 1/T Eq. (9) (Fig. 10) and the thermodynamic parameters were summarized in Table 4.

As shown, all of ΔG° values were found to be negative at various temperatures, confirming the spontaneous nature of the adsorption process[10, 64]. In addition, the ΔG° values became less negative at higher temperatures making the adsorption less favourable due to the weakening of the adsorbent-adsorbate bonds[9]. ΔG° for MB adsorption on the investigated adsorbents in the range -6.1324 to -18.8487 kJ/mol indicates a physical adsorption process where, the change of free energy for physical adsorption is generally between -20 and 0 kJ/mol, the physical adsorption together with chemical adsorption is in the range of -20 to -80 kJ/mol and chemical adsorption is at a range of -80 to -400 kJ/mol[5, 65].

The negative values of ΔH° indicate the exothermic nature of the adsorption process[66, 67], and this explains the decline in adsorptive performance at elevated temperatures[9]. The negative values of ΔS° for adsorption suggest less randomness of MB near the surface of adsorbents[66, 68] which suggest that the process may be reversible in nature.

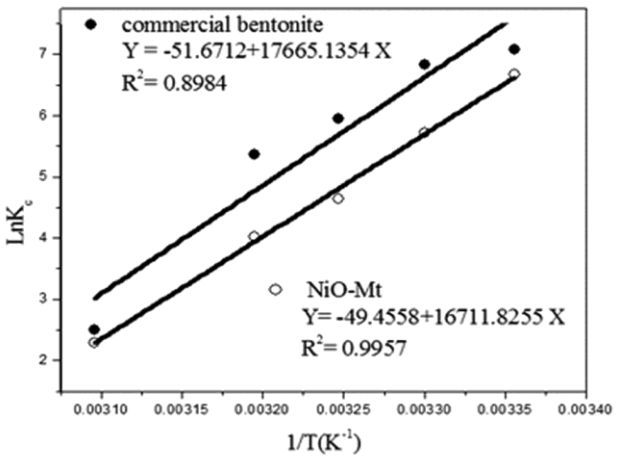

Fig. 10 — Thermodynamics analysis for MB adsorption by commercial bentonite and NiO-Mt

Conclusion

In order to test and compare the adsorption capability, both of commercial bentonite and NiO-Mt were used to remove MB from aqueous solution. NiO-Mt was synthesized and characterised by FTIR, XRF and XRD analysis. The operating parameters for the maximum adsorption were contact time (10 min), adsorbent mass (25 mg), dye solution concentration (100 mg/L), natural pH of the solution (6.3 and 5.8 for commercial bentonite and NiO-Mt, respectively) and temperature (298 K) were set for both adsorbents. Removal of methylene blue was pH independent with commercial bentonite, while for NiO-Mt, the maximum removal was attained at pH from 5.8 and 11. The MB adsorption onto both adsorbents can be described using pseudo-second order kinetics model with good determination coefficient. The equilibrium results fitted mainly with the Langmuir model. The negative values of ΔG° and ΔH° indicate that the adsorption process was physical, spontaneous and exothermic. Based on the present investigation, it could be concluded that the modified local montmorillonite (NiO-Mt) adsorbent prepared can be used efficiently in the removal of MB from aqueous solutions, and we encourage the generalization of its use in the Algeria's industries.

Acknowledgement

The authors are grateful to Mrs Zineb KAHLERRAS « département pédagogique sécurité industrielle et environnement de l'IAP Boumerdès » for FTIR analysis. The authors also acknowledge Pr Faiza ZERMANE « Laboratoire de chimie physique des interfaces des matériaux appliqués à l'environnement » at Blida University for XRD analysis.

Supplementary Information

Supplementary information is available on the website http://nopr.niscpr.res.in/handle/123456789/55.

References

1 Şahin Ö, Kaya M & Saka C, *Appl Clay Sci*, 116 (2015) 46.
2 Pandey R L M, *Appl Clay Sci*, 169 (2019) 102.
3 Huang Z, Li Y, Chen W, Shi J, Zhang N, Wang X, Li Z, Gao L & Zhang Y, *Mater Chem Phys*, 202 (2017) 266.
4 Fan S, Wang Y, Wang Z, Tang J, Tang J & Li X, *J Environ Chem Eng*, 5 (2017) 601.
5 Hassan A F & Elhadidy H, *J Environ Chem Eng*, 5 (2017) 955.
6 Hassan A F, Abdel-Mohsen A M & Moustafa M G F, *Carbohydr Polym*, 102 (2014) 192.
7 Pathania D, Sharma S & Singh P, *Arab J Chem*, 10 (2017) S1445.
8 Li X, Wang S, Liu Y, Jiang L, Song B, Li M, Zeng G, Tan X, Cai X & Ding Y, *J Chem Eng Data*, 62 (2017) 407.
9 De Castro M L F A, Abad M L B, Sumalinog D A G, Abarca R R M, Paoprasert P & De Luna M D G, *Sust Environ Res*, 28 (2018) 197.
10 Abuhatab S, El-Qanni A, Al-Qalaq H, Hmoudah M & Al-Zerei W, *J Environ Manage*, 268 (2020) 110713.
11 Abidi N, Errais E, Duplay J, Berez A, Jrad A, Schäfer G, Ghazi M, Semhi K & Trabelsi-Ayadi M, *J Clean Prod*, 86 (2015) 432.
12 Kurniawan A, Sutiono H, Ju Y H, Soetaredjo F E, Ayucitra A, Yudha A & Ismadji S, *Microporous Mesoporous Mater*, 142 (2011) 184.
13 Hajjaji M & El Arfaoui H, *Appl Clay Sci*, 46 (2009) 418.
14 Dinçer A R, Güneş Y & Karakaya N, *J Hazard Mater*, 141 (2007) 529.
15 Aghdasinia H & Asiabi H R, *Environ Earth Sci*, 77 (2018) 1.
16 Bayram T, Bucak S & Ozturk D, *Chem Eng Process: Process Intensif*, 158 (2020) 108.
17 Haounati R, Ouachtak H, El Haouti R, Akhouairi S, Largo F, Akbal F, Benlhachemi A, Jada A & Ait Addi A, *Sep Purif Technol*, 255 (2021) 117335.
18 Jawad A H & Abdulhameed A S, *Surf Interfaces*, 18 (2020) 100422.
19 Esvandi Z, Foroutan R, Peighambardoust S J, Akbari A & Ramavandi B, *Surf Interfaces*, 21 (2020) 100754.
20 Ali N, Ali F, Ullah I, Ali Z, Duclaux L, Reinert L, Lévêque J M, Farooq A, Bilal M & Ahmad I, *Environ Technol Innov*, 19 (2020) 101001.
21 Bueno S, Durán E, Gámiz B & Hermosín M C, *J Environ Chem Eng*, 9 (2021) 104623.
22 Chaari I, Medhioub M, Jamoussi F & Hamzaoui A H, *J Mol Struct*, 1223 (2020) 128944.
23 Kadhum S T, Yassen A G & Albayati T M, *J Chem Eng*, 36 (2021) 19.
24 Ullah R, Jan I F, Ajmal M, Shah A, Akhter M S, Ullah H & Waseem A, *Pol J Environ Stud*, 29 (2020) 3831.
25 Alorabi A Q, Shamshi H M, Mahboob A M, Zabin S A, Alsenani N I & Essam B N, *Nanomater*, 11 (2021) 2789.
26 Saeed M, Munir M, Nafees M, Ahmad S S S, Ullah H & Waseem A, *Microporous Mesoporous Mater*, 291 (2020) 109697.
27 Khalaf H, Bouras O & Perrichon V, *Microporous Mesoporous Mater*, 8 (1997) 141.
28 Ferro-Garcia M A, Rivera-Utrilla J, Bautista-Toledo I & Moreno-Castilla C, *Langmuir*, 14 (1998) 1880.
29 Dutta D & Dutta D K, *Appl Catal A: Gen*, 487 (2014) 158.
30 Boukhatem H, Khalaf H, Djouadi L, Gonzalez F V, Navarro R M, Santaballa J A & Canle Lopez M, *Appl Catal B*, 211 (2017) 114.
31 Abukhadra M R, Sayed M A, Rabie A M & Ahmed S A, *Colloids Surf A*, 577 (2019) 583.
32 Rabie A M, Shaban M, Abukhadra M R, Hosney R, Ahmed S A & Negm N A, *J Mol Liq*, 278 (2019) 224.
33 Lei C, Pi M, Cheng B, Jiang C & Qin J, *Appl Surf Sci*, 435 (2018) 1002.
34 Niu H, Zhou D, Yang X, Li X, Wang Q & Qu F, *J Mater Chem A*, 3 (2015) 18413.
35 Motahari F, Mozdianfard M R & Salavati-Niasari M, *Process Saf Environ Prot*, 93 (2015) 282.
36 Gao X, Mao H, Lu M, Yang J & Li B, *Microporous Mesoporous Mater*, 148 (2012) 25.
37 Modiba E, Enweremadu C & Rutto H, *Chin J Chem Eng*, 23 (2015) 281.
38 Xiao J, Peng T, Dai K, Zan L & Peng Z, *J Solid State Chem*, 180 (2007) 3188.
39 Wang R, Li Q, Xie D, Xiao H & Lu H, *Appl Surf Sci*, 279 (2013) 129.
40 Jiang Y, Huang T, Dong L, Su T, Li B, Luo X, Xie X, Qin Z, Xu C & Ji H, *Catalysts*, 8 (2018) 646.
41 Kumar A & Lingfa P, *Mater Today: Proc*, 22 (2020) 737.
42 Lu X, Gu F, Liu Q, Gao J, Liu Y, Li H, Jia L, Xu G, Zhong Z & Su F, *Fuel Process Technol*, 135 (2015) 34.
43 Farzaneh F & Haghshenas S, *Mater Sci Appl*, 3 (2012) 697.
44 Meng B, Guo Q, Men X, Ren S, Jin W & Shen B, *J Saudi Chem Soc*, 24 (2020) 334.
45 Atta A M, Al-Lohedan H A, Al Othman Z A, Abdel-Khalek A A & Tawfeek A M, J *Ind Eng Chem*, 31 (2015) 374.
46 Chang J, Ma J, Ma Q, Zhang D, Qiao N, Hu M & Ma H, *Appl Clay Sci*, 119 (2016) 132.
47 Fan H, Zhou L, Jiang X, Huang Q & Lang W, *Appl Clay Sci*, 95 (2014) 150.
48 Zhou Q, Gao Q, Luo W, Yan C, Jia Z & Duan P, *Colloids Surf A : Physicochem Eng Asp*, 470 (2015) 258.
49 Ho Y S & McKay G, *Trans I Chem E Part B*, 76 (1998) 183.
50 Ho Y S & McKay G, *Process Biochem*, 34 (1999) 451.
51 Abbad B & Lounis A, *Desalin Water Treat*, 52 (2014) 7766.
52 Pandimurugan R & Thambidurai S, *J Environ Chem Eng*, 4 (2016) 1332.
53 Akpomie K G, Dawodu F A & Adebowale K O, *Alex Eng J*, 54 (2015) 757.
54 Narine D R & Guy R D, *Clays Clay Miner*, 29 (1981) 205.

55 Bilgic C, *J Colloid Interface sci*, 281 (2005) 33.
56 Rezala H, Douba H, Boukhatem H & Romero A, *J Chem Soc Pak*, 42 (2020) 550.
57 Sun Y, Wu Z Y, Wang X, Ding C, Cheng W, Yu S H & Wang X, *Environ Sci Technol*, 50 (2016) 4459.
58 Ebrahim S E, Sulaymon A H & Saad A H, *Desalin Water Treat*, 57 (2016) 20915.
59 Tarek M E, Uyiosa O A, Kingsley E U, Robert B O, Mohamed A E, Mohamed A H, Safaa R, Otolorin A O & Ahmed E, *Biomass Convers Biorefin*, (2022).
60 Barka N, Qouzal S, Assabbane A, Noinhan A & Ichou Y A, *J Saudi Chem Soc*, 15 (2011) 263.
61 Dogan M, Alkan M, Demirbas O, Özdemir Y & Özmetin C, *Chem Eng J*, 124 (2006) 89.
62 Almeida C A P, Debacher N A, Downs A J, Cottet L & Mello C A D, *J Colloid Interface Sci*, 332 (2009) 46.
63 Zhang K, Li H, Xu X & Yu H, *Microporous Mesoporous Mater*, 255 (2018) 7.
64 El-Qanni A, Nassar N N & Vitale G, *Chem Eng J*, 327 (2017) 666.
65 Baseri J R, Palanisamy P N & Kumar P S, *Indian J Chem Technol*, 19 (2012) 311.
66 Mohamed E M, Gehan M N, Nabila M E, Heba I B, Sandeep K & Tarek M A, *J Ind Eng Chem*, 37 (2016) 156.
67 Demirbas A, Sari A & Isldak O, *J Hazard Mater*, 135 (2006) 226.
68 Leilei L, Feng L, Huimin D, Xiaojiao W, Jianbo L, Yanhui W & Chuannan L, *Colloids Surfaces B: Biointerfaces*, 141 (2016) 253.